01 Mar 2015

The Loss of Hh Responsiveness by a Non-Ciliary Gli2 Variant

Jinling Liu
Missouri University of Science and Technology, jinling.liu@mst.edu

Huiqing Zeng

Aimin Liu

© 2015. Published by The Company of Biologists Ltd | Development (2015) 142, 1651-1660 doi:10.1242/dev.119669

RESEARCH ARTICLE

The loss of Hh responsiveness by a non-ciliary Gli2 variant

Jinling Liu[1], Huiqing Zeng[1] and Aimin Liu[1,2,*]

ABSTRACT

Hedgehog signaling is crucial for vertebrate development and physiology. Gli2, the primary effector of Hedgehog signaling, localizes to the tip of the primary cilium, but the importance of its ciliary localization remains unclear. We address the roles of Gli2 ciliary localization by replacing endogenous Gli2 with Gli2$^{\Delta CLR}$, a Gli2 variant not localizing to the cilium. The resulting *Gli2*$^{\Delta CLRKI}$ and *Gli2*$^{\Delta CLRKI}$*;Gli3* double mutants resemble *Gli2*-null and *Gli2;Gli3* double mutants, respectively, suggesting the lack of Gli2$^{\Delta CLR}$ activation in development. Significantly, Gli2$^{\Delta CLR}$ cannot be activated either by pharmacochemical activation of Smo *in vitro* or by loss of *Ptch1 in vivo*. Finally, Gli2$^{\Delta CLR}$ exhibits strong transcriptional activator activity in the absence of Sufu, suggesting that the lack of its activation *in vivo* results from a specific failure in relieving the inhibitory function of Sufu. Our results provide strong evidence that the ciliary localization of Gli2 is crucial for cilium-dependent activation of Hedgehog signaling.

KEY WORDS: Cilium, Hedgehog signaling, Mouse, Spinal cord, Sufu

INTRODUCTION

The Hedgehog (Hh) family of secreted proteins mediates numerous inductive events crucial for the proliferation, differentiation and migration of cells in diverse species ranging from planarian to fruit flies and vertebrates (Briscoe and Thérond, 2013; Ye and Liu, 2011). Studies in the past decade suggest that Hh signaling in vertebrates requires the primary cilium, a solitary protrusion on the surface of most somatic cells implicated in a plethora of human genetic diseases (Goetz and Anderson, 2010; Nozawa et al., 2013). However, the molecular mechanisms underlying the connection between the cilium and Hh signal transduction remain enigmatic.

The vertebrate Hh family of proteins, including Shh, Ihh and Dhh, interacts with the Patched (Ptch) receptors, especially Ptch1 (Briscoe and Thérond, 2013). This interaction relieves the inhibition on a G protein-coupled receptor-like protein Smoothened (Smo), and inhibits the proteolytic processing of zinc-finger transcription factors Gli2 and Gli3 into repressors. Moreover, high levels of Hh pathway activation convert the full-length Gli2 and Gli3 into labile activators, possibly through dissociating them from their negative regulator suppressor of fused (Sufu) (Humke et al., 2010; Lin et al., 2014; Tukachinsky et al., 2010). A third member of the Gli family, Gli1, is expressed in response to the initial activation of the Hh pathway, bolstering the pathway activation to a higher level.

Hh pathway activation coincides with the exclusion of Ptch1 from, and concomitant accumulation of Smo in, the primary cilium (Corbit et al., 2005; Rohatgi et al., 2007). The ciliary accumulation of Smo appears to be essential, but not sufficient, for its activation (Corbit et al., 2005; Rohatgi et al., 2009; Wang et al., 2009; Wilson et al., 2009). All mammalian Gli proteins, as well as Sufu, localize to the tip of the cilium in a coordinated process, which is further enhanced by Hh signaling (Chen et al., 2009; Haycraft et al., 2005; Wen et al., 2010; Zeng et al., 2010b). Disturbing the cytoplasmic microtubule network or intraflagellar transport (IFT) has been shown to reduce Gli2 ciliary localization and coincidently disrupt Hh signaling (Keady et al., 2012; Kim et al., 2009). However, as cytoskeleton and IFT affect the localization of numerous other cellular components, these approaches have not adequately established a connection between Gli2 ciliary localization and Hh pathway activation.

The molecular mechanisms of Gli activation have been the focus of inquiry in recent years. cAMP-dependent protein kinase (PKA) is an essential negative regulator of Gli proteins (Niewiadomski et al., 2014; Tuson et al., 2011). However, the pathway activation in the absence of PKA is dependent on the cilium, suggesting that additional cilium-dependent mechanisms exist downstream of PKA inhibition to allow Gli activation (Tuson et al., 2011). By contrast, the removal of Sufu leads to Gli activation even in the absence of the cilium, and the dissociation between Sufu and Gli proteins appear to be dependent on the cilium (Chen et al., 2009; Humke et al., 2010; Jia et al., 2009). These results suggest that the release of Gli proteins from Sufu inhibition in the cilium is a major event in Gli activation.

Here, we report that a Gli2 variant, Gli2$^{\Delta CLR}$, fails to localize to the cilium, but retains intrinsic transcriptional activity and responds to Sufu inhibition. To determine whether the ciliary localization is required for Gli2 activation, we generated a *Gli2*$^{\Delta CLR}$ knock-in mouse strain in which *Gli2*$^{\Delta CLR}$ is transcribed in a similar pattern to endogenous *Gli2*. We show that Hh signaling is compromised in *Gli2*$^{\Delta CLRKI}$ homozygous and *Gli2*$^{\Delta CLRKI/-}$ transheterozygous mutants, and is further reduced in *Gli2*$^{\Delta CLRKI}$*; Gli3* double mutants, suggesting that Gli2$^{\Delta CLR}$ is not properly activated in development. Supporting the hypothesis that Gli2 ciliary localization is required for its activation by the Hh pathway, both *in vitro* pharmacochemical activation of Smo and *in vivo* loss of *Ptch1* mutation fail to activate Gli2$^{\Delta CLR}$. Finally, we demonstrate that Gli2$^{\Delta CLR}$ is as capable as endogenous Gli2 at activating Hh target genes in the absence of Sufu, suggesting that the lack of its activation *in vivo* results from a failure in its cilium-dependent release from Sufu inhibition by Hh signaling.

RESULTS

Removing mouse Gli2 from the primary cilium without disrupting its intrinsic transcriptional activity and response to Sufu

One way to specifically test the role of Gli2 ciliary localization in Hh pathway activation is to determine whether a Gli2 variant that does not localize to the cilium can be activated by Hh signaling. To accomplish this goal, it is essential to make sure that the intrinsic transcriptional activity of Gli2 is not disrupted by the mutation that

[1]Department of Biology, Eberly College of Science, The Pennsylvania State University, University Park, PA 16802, USA. [2]Center for Cellular Dynamics, Huck Institute of Life Sciences, The Pennsylvania State University, University Park, PA 16802, USA.

*Author for correspondence (axl25@psu.edu)

Received 9 November 2014; Accepted 9 March 2015

Development (2015) 142, 1651-1660 doi:10.1242/dev.119669

removes the protein from the cilium. The intrinsic transcriptional activity of Gli2 can be revealed by overexpression because previous studies indicated that overexpression of Gli1 or Gli2 overrides the inhibitory function of Sufu and activates Hh-target genes independent of the cilium (Chen et al., 2009; Jia et al., 2009). We have found that a central region of mouse Gli2 (residues 570 to 967, the ciliary localization region, CLR), immediately downstream of the zinc-finger DNA-binding domains, was required for the localization of Gli2 to the tip of the primary cilium (Fig. 1A; Zeng et al., 2010b). Consistent with our previous results, we found that the green fluorescent protein (GFP)-tagged Gli2, but not the variant lacking the CLR, namely Gli2$^{\Delta CLR}$, localized to the tips of the cilia in mouse embryonic fibroblasts (MEFs) (Fig. 1B,C). In addition, we found that GFP-Gli2 localized to both the nucleus and cytoplasm, whereas GFP-Gli2$^{\Delta CLR}$ localized predominantly to the cytoplasm (Fig. 1B,D). We induced Hh signaling by treating the cells with Smo agonist (SAG). Although the efficient GFP-Gli2 ciliary localization in DMSO-treated cells (100% of 51 cells) prevented a further increase in the percentage of SAG-treated cells exhibiting GFP-Gli2 ciliary localization (100% of 50 cells), we did observe an increase in the amount of GFP-Gli2 at the ciliary tips when judged by the fluorescence intensity (Fig. 1B,C). By contrast, SAG treatment failed to induce the ciliary localization of GFP-Gli2$^{\Delta CLR}$ (Fig. 1B,C). Interestingly, SAG treatment appeared to result in a slight decrease in the nuclear localization of GFP-Gli2, but in no appreciable change in the predominant distribution of GFP-Gli2$^{\Delta CLR}$ in the cytoplasm (Fig. 1B,D).

Since the repressor, activator and DNA-binding domains were all intact in Gli2$^{\Delta CLR}$, we expected Gli2$^{\Delta CLR}$ to retain intrinsic transcriptional activity. To test this, we overexpressed various amounts of GFP-tagged Gli2 and Gli2$^{\Delta CLR}$ in Shh-L2 cells that stably express a Gli-responsive luciferase reporter gene (Taipale et al., 2000), and found that GFP-Gli2$^{\Delta CLR}$ activated the reporter gene expression more efficiently than GFP-Gli2, suggesting that the removal of CLR did not disrupt the intrinsic activator activity of Gli2 (Fig. 1E). The extra activity of GFP-Gli2$^{\Delta CLR}$ could result from its increased stability because the CLR includes sites that are required for SCF$^{\beta TRCP}$-mediated degradation of Gli2 (Pan et al., 2006). However, our immunoblot analysis suggested that the difference between the levels of GFP-Gli2$^{\Delta CLR}$ and GFP-Gli2 (<25%; Fig. 1F) could not explain the more than fivefold difference in activity. Therefore, we conclude that GFP-Gli2$^{\Delta CLR}$ exhibits higher intrinsic transcriptional activator activity than GFP-Gli2.

Sufu is an essential negative regulator of Gli2 and cilium-dependent relief of Gli2 from Sufu inhibition is a crucial event in Hh pathway activation (Chen et al., 2009; Cooper et al., 2005; Humke et al., 2010; Jia et al., 2009; Svärd et al., 2006; Tukachinsky et al., 2010). Consistent with our previous co-immunoprecipitation analysis that showed physical interaction between Sufu and Gli2$^{\Delta CLR}$ (Zeng et al., 2010b), we found that overexpression of Sufu inhibits reporter expression activated by Gli2$^{\Delta CLR}$, suggesting that Gli2$^{\Delta CLR}$ remains sensitive to Sufu inhibition (Fig. 1G).

Replacement of Gli2 with Gli2$^{\Delta CLR}$ *in vivo* through a knock-in approach

As Gli2$^{\Delta CLR}$ lacks ciliary localization, but retains its intrinsic transcriptional activity and its response to Sufu inhibition, we reasoned that Gli2$^{\Delta CLR}$ could be used to test the hypothesis that the

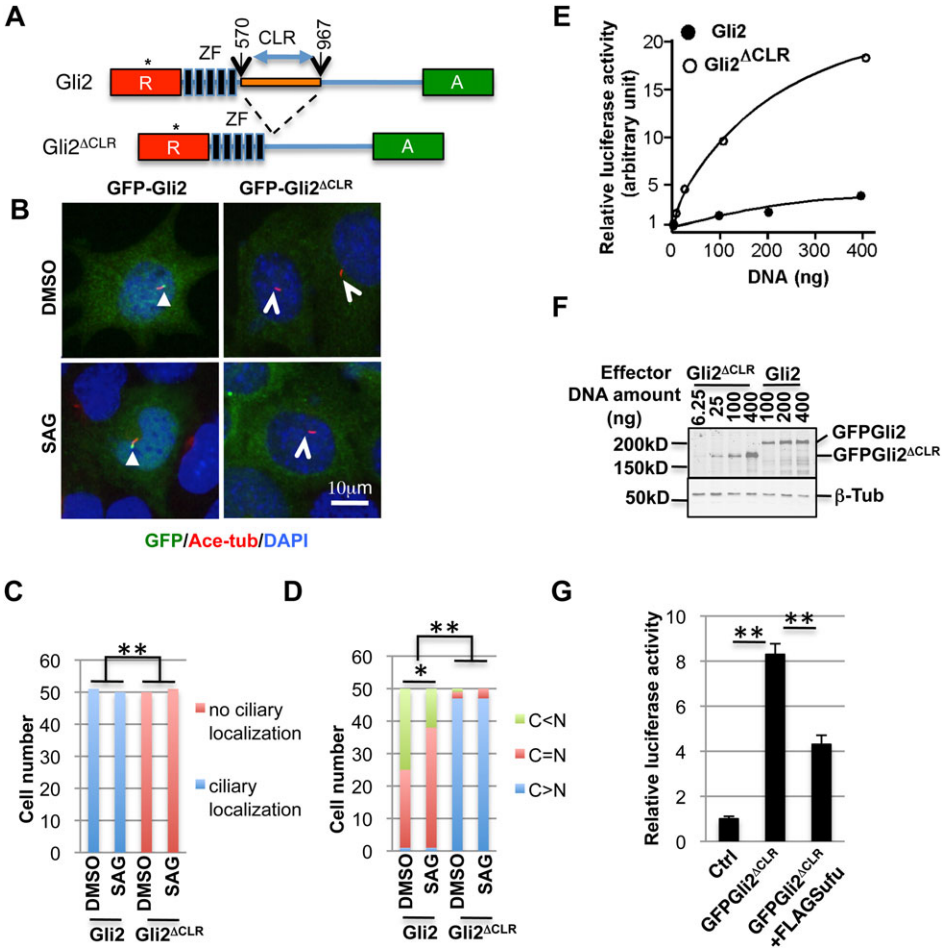

Fig. 1. The non-ciliary Gli2$^{\Delta CLR}$ retains intrinsic transcriptional activity and response to Sufu. (A) A schematic illustration of Gli2 and Gli2$^{\Delta CLR}$. Red and green boxes denote the repressor (R) and activator (A) domains, respectively. ZF, zinc-finger DNA-binding domain. Numbers indicate the position of the ciliary localization region (CLR), which is highlighted in orange. Asterisks indicate the locations for the primers used in the qRT-PCR reactions presented in Fig. 2B. (B) Representative images of GFP-Gli2 and GFP-Gli2$^{\Delta CLR}$-expressing MEFs treated with DMSO or Smo agonists (SAG). Acetylated α-Tubulin reveals the cilia and DAPI reveals the nuclei. The arrowheads indicate the tips of the cilia. (C) Statistical analysis of the ciliary localization of GFP-Gli2 and GFP-Gli2$^{\Delta CLR}$. $^{**}P=7\times10^{-46}$, χ^2-test. (D) Statistical analysis of the nuclear/cytoplasmic localization of GFP-Gli2 and GFP-Gli2$^{\Delta CLR}$. $^{*}P=0.026$, $^{**}P=3\times10^{-19}$, χ^2-test. (E) GFP-Gli2$^{\Delta CLR}$ activates the expression of a Gli-responsive reporter more efficiently than GFP-Gli2. *x*-axis: amount of effector DNA used for transfection. *y*-axis: relative luciferase reporter expression, control sample without effector transfection is set to 1. (F) Immunoblot analysis on samples used for the experiment in E. (G) Sufu inhibits Gli2$^{\Delta CLR}$-activated expression of a Gli-responsive reporter. For E-G, three independent experiments were performed and each experiment was carried out in triplicate. $^{**}P<0.01$, unpaired Student's *t*-test.

Development (2015) 142, 1651-1660 doi:10.1242/dev.119669

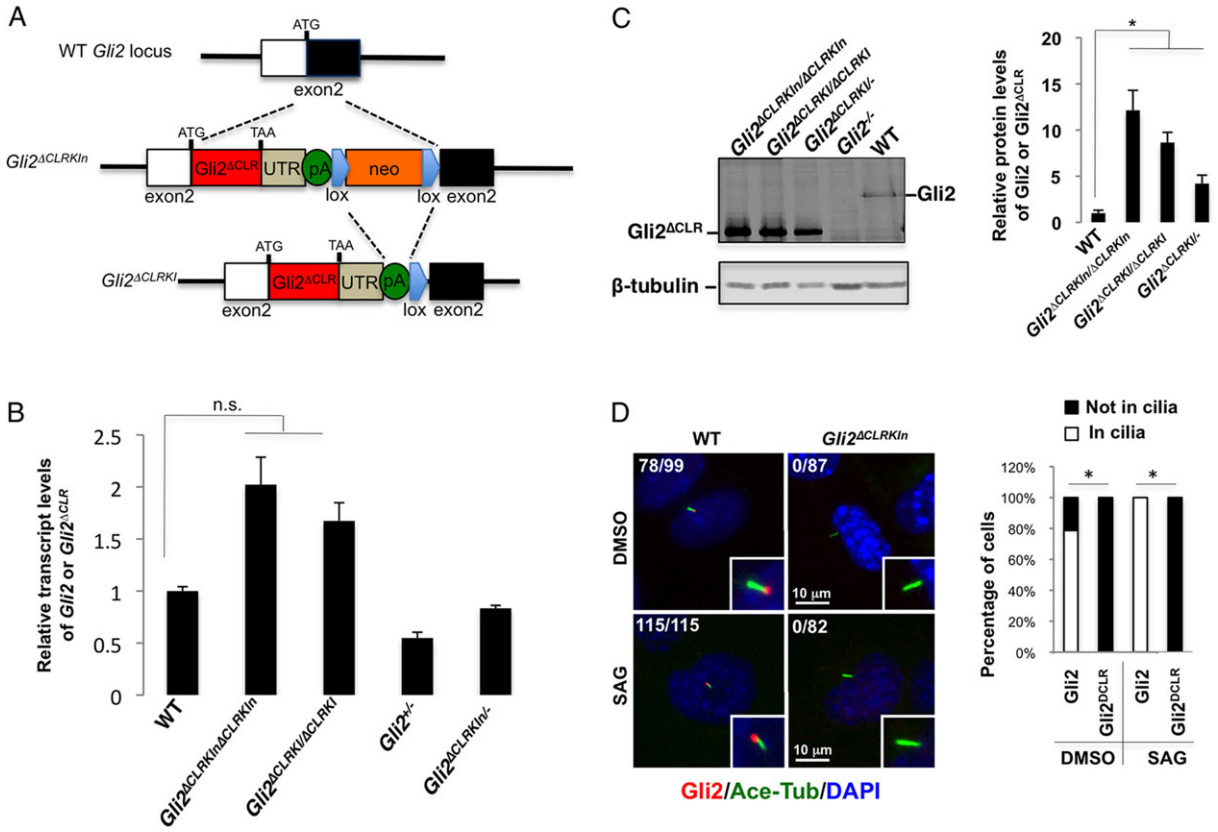

Fig. 2. Replacing endogenous Gli2 with Gli2$^{\Delta CLR}$. (A) The two knock-in alleles used in this study. In *Gli2*$^{\Delta CLRKIn}$, the open reading frame of Gli2$^{\Delta CLR}$, along with the 3′ untranslated region (UTR) of *Gli2* and three tandem repeats of SV40 polyA sequence (pA), replaces 111 bp in the first coding exon of *Gli2*, followed with a neomycin expression cassette (neo) flanked with loxP sites. In *Gli2*$^{\Delta CLRKI}$, recombination between the two loxP sites removes the neo cassette, leaving a single loxP site. (B) qRT-PCRs of RNA extracted from E9.5 whole embryos show comparable transcript levels between wild type and the *Gli2*$^{\Delta CLR}$ knock-in alleles. n.s., $P>0.05$, unpaired Student's *t*-test. $n=3$ embryos for each genotype. (C) Immunoblot analysis on E9.5 whole-embryo lysates shows an increase in the level of the Gli2$^{\Delta CLR}$ protein in *Gli2*$^{\Delta CLR}$ knock-in embryos compared with endogenous Gli2. *$P<0.05$, unpaired Student's *t*-test. (D) Immunofluorescence analysis of starved mouse embryonic fibroblasts confirmed that Gli2$^{\Delta CLR}$ did not localize to the cilium, even in the presence of Smo agonist (SAG). Cilia are labeled with acetylated α-Tubulin. Nuclei are labeled with DAPI. *$P<0.05$, χ^2-test.

ciliary localization of Gli2 was essential for Hh pathway activation. Previous studies have indicated that Gli overexpression overrides the inhibitory function of Sufu and activates Hh target genes independently of the cilium (Chen et al., 2009; Jia et al., 2009). Therefore, Gli2$^{\Delta CLR}$ needs to be expressed at a near physiological level to address whether the lack of its ciliary localization affects its activation by Hh signaling. Therefore, we replaced endogenous *Gli2* with *Gli2*$^{\Delta CLR}$ *in vivo* through a gene targeting-based 'knock-in' approach in mouse embryonic stem (ES) cells such that the transcription of *Gli2*$^{\Delta CLR}$ is under the native transcriptional cis-regulatory elements of the *Gli2* locus. Previous studies have shown that genes 'knocked in' to the same location were expressed in similar patterns to that of endogenous *Gli2* (Bai and Joyner, 2001; Bai et al., 2004).

In our knock-in DNA construct, ~110 bp of the first coding exon of *Gli2* (from 73 bases upstream to 38 bases downstream of endogenous translational start) were replaced with the coding sequence for *Gli2*$^{\Delta CLR}$ followed with the entire 3′ untranslated region of *Gli2* and three tandem repeats of 250 bp of SV40 polyA signal (Fig. 2A; supplementary material Fig. S1A). A neomycin-resistance gene expression cassette (neo) flanked with *loxP* sites was also inserted to enable drug selection of the correctly targeted ES cells. We derived *Gli2*$^{\Delta CLRKIn}$ mice from two independently targeted ES cell clones, and confirmed the predicted integration of the targeting constructs into the *Gli2* locus through Southern hybridization and polymerase chain reaction (PCR) (supplementary material Fig. S1B-E).

To confirm that the levels of *Gli2*$^{\Delta CLR}$ transcription in *Gli2*$^{\Delta CLR}$ knock-in embryos were comparable with that of endogenous *Gli2*, we performed quantitative real-time reverse transcriptase PCR analysis (qRT-PCR) on embryonic day 9.5 (E9.5) embryos. We found that the level of *Gli2*$^{\Delta CLR}$ mRNA in *Gli2*$^{\Delta CLRKIn/\Delta CLRKIn}$ embryos was nearly twice as much as that of endogenous *Gli2* (Fig. 2B). Strikingly, immunoblot analysis of *Gli2*$^{\Delta CLRKIn/\Delta CLRKIn}$ embryos showed a ~12-fold increase in the level of Gli2$^{\Delta CLR}$ protein compared with that of Gli2 in wild-type embryos (Fig. 2C). We subsequently removed neo^R by breeding *Gli2*$^{\Delta CLRKIn/+}$ mice to a mouse line expressing Cre recombinase in the germline. The levels of the mRNA (~70% more than *Gli2*) and protein (~8.7-fold of Gli2) for Gli2$^{\Delta CLR}$ in resulting *Gli2*$^{\Delta CLRKI/\Delta CLRKI}$ homozygous mutants were slightly lower than that in *Gli2*$^{\Delta CLRKIn/\Delta CLRKIn}$ mutant embryos, but the difference was not statistically significant (Fig. 2B,C).

To make the Gli2$^{\Delta CLR}$ protein level more comparable with endogenous Gli2, we generated transheterozygous embryos by breeding *Gli2*$^{\Delta CLRKIn/+}$ or *Gli2*$^{\Delta CLRKI/+}$ heterozygotes to the carriers of a null allele of *Gli2* (*Gli2*$^{tm2.1Alj}$; Bai and Joyner, 2001). For simplicity, we will refer to it as *Gli2*$^{-}$. As expected, in *Gli2*$^{\Delta CLRKIn/-}$ and *Gli2*$^{\Delta CLRKI/-}$ transheterozygous embryos, *Gli2*$^{\Delta CLR}$ was transcribed at a slightly lower (~80%) level than that of endogenous *Gli2* in wild-type littermates (Fig. 2B). Consistently, the level of Gli2$^{\Delta CLR}$

Development (2015) 142, 1651-1660 doi:10.1242/dev.119669

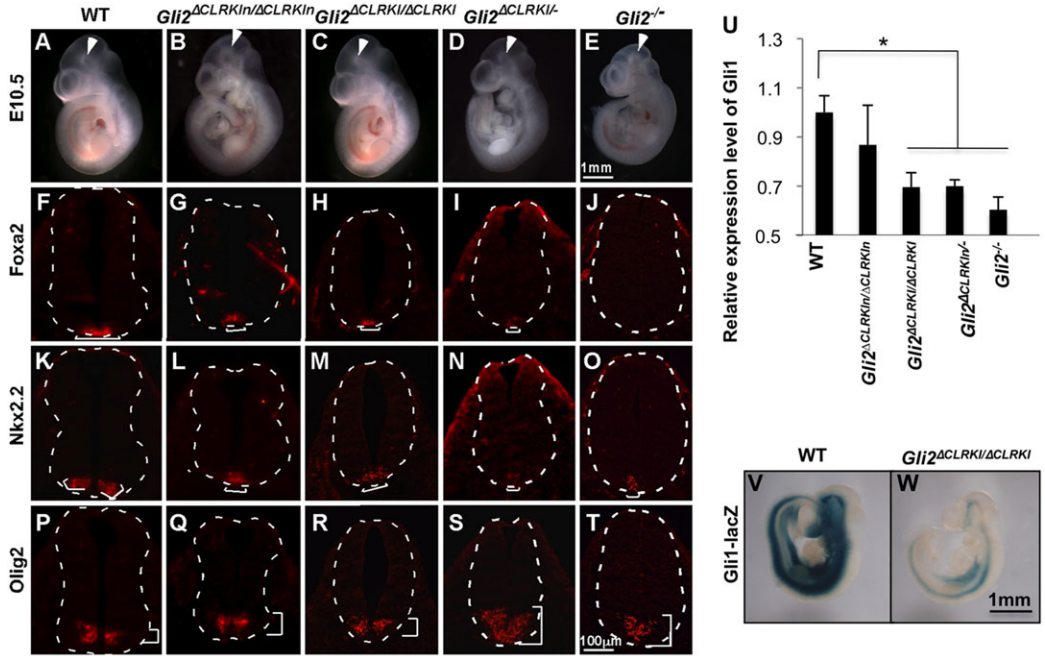

Fig. 3. Abnormal ventral spinal cord patterning and compromised Hh signaling in *Gli2*$^{\Delta CLR}$ knock-in mutants. (A-E) Lateral views of E10.5 whole embryos. Arrowheads indicate the mesencephalic flexure. (F-T) Immunofluorescence images of the E10.5 spinal cords at the thoracic level. Similar patterns were observed in more posterior regions. Dashed lines outline the spinal cords. Brackets show the expression domains. (F-I) *Foxa2* expression is reduced in the *Gli2*$^{\Delta CLRKIn/\Delta CLRKIn}$ (n=4), *Gli2*$^{\Delta CLRKI/\Delta CLRKI}$ (n=3) and *Gli2*$^{\Delta CLRKIn/-}$ (n=4) mutant spinal cords. (J) *Foxa2* expression is absent in *Gli2*$^{-/-}$ (n=3) mutant embryos. (K-O) *Nkx2.2* expression is in the ventral midline of the *Gli2*$^{\Delta CLRKIn/\Delta CLRKIn}$ (n=4), *Gli2*$^{\Delta CLRKI/\Delta CLRKI}$ (n=3), *Gli2*$^{\Delta CLRKIn/-}$ (n=4) and *Gli2*$^{-/-}$ mutant spinal cords (n=3). (P-T) *Olig2* expression is expanded ventrally in the *Gli2*$^{\Delta CLRKIn/\Delta CLRKIn}$ (n=4) and *Gli2*$^{\Delta CLRKI/\Delta CLRKI}$ (n=3) mutant spinal cords, and is expanded to the ventral midline in the *Gli2*$^{\Delta CLRKIn/-}$ (n=4) and *Gli2*$^{-/-}$ (n=3) mutant spinal cords. (U) Relative expression levels of *Gli1* in E9.5 embryos measured with qRT-PCR. n=3 for each genotype. *P<0.05, unpaired Student's t-test. (V,W) X-gal-stained E9.5 embryos showing reduced *Gli1-lacZ* expression in *Gli2*$^{\Delta CLRKI/\Delta CLRKI}$;*Gli1*$^{lacZ/+}$ embryos (n=2) compared with *Gli1*$^{lacZ/+}$ embryos (n=5).

protein in the transheterozygotes is approximately four times as much as that of endogenous Gli2 protein in wild-type embryos (Fig. 2C).

We next examined the subcellular localization of Gli2$^{\Delta CLR}$ in *Gli2*$^{\Delta CLRKIn/\Delta CLRKIn}$ homozygous mutant mouse embryonic fibroblasts (MEFs) through immunofluorescence. Using an antibody against the N-terminal 416 amino acids of Gli2, we found that wild-type Gli2, but not Gli2$^{\Delta CLR}$, localizes to the tips of the primary cilia (Fig. 2D). Treating the wild-type cells with Smo agonist (SAG) resulted in an increase in Gli2 accumulation at the tips of the cilia (Fig. 2D). By contrast, Gli2$^{\Delta CLR}$ remains absent from the cilia upon SAG treatment (Fig. 2D).

Abnormal patterning and compromised Hh signaling in the Gli2$^{\Delta CLR}$ knock-in mutant spinal cords

Both *Gli2*$^{\Delta CLRKIn/+}$ and *Gli2*$^{\Delta CLRKI/+}$ heterozygous mice are viable and fertile, and do not exhibit any noticeable morphological or behavioral defects. However, we did not recover any *Gli2*$^{\Delta CLRKIn/\Delta CLRKIn}$ and *Gli2*$^{\Delta CLRKI/\Delta CLRKI}$ homozygotes or *Gli2*$^{\Delta CLRKI/-}$ transheterozygotes at weaning, suggesting that Gli2$^{\Delta CLR}$ was incompatible with postnatal survival.

At E10.5, *Gli2*$^{\Delta CLRKIn/\Delta CLRKIn}$ and *Gli2*$^{\Delta CLRKI/\Delta CLRKI}$ homozygous and *Gli2*$^{\Delta CLRKI/-}$ transheterozygous mutant embryos exhibit kinked mesencephalic flexure morphology (compare Fig. 3A-D) that is highly reminiscent of *Gli2*-null homozygous mutants (Fig. 3E). Gli2 plays an important role in the induction of the floor plate and V3 interneurons of the mouse spinal cord (Ding et al., 1998; Matise et al., 1998). Therefore, we examined the ventral spinal cord patterning of these embryos to determine whether Gli2$^{\Delta CLR}$ exhibits full activity of Gli2 in development. *Foxa2* was expressed strongly in the floor plate of wild-type spinal cord (Fig. 3F). We found fewer *Foxa2*-expressing cells in the *Gli2*$^{\Delta CLRKIn/\Delta CLRKIn}$ homozygous mutant spinal cords (Fig. 3G). *Nkx2.2*-expressing V3 interneuron progenitors were normally located lateral to the floor plate (Fig. 3K). A reduced number of *Nkx2.2*-expressing cells were present in the ventral midline of the *Gli2*$^{\Delta CLRKIn/\Delta CLRKIn}$ homozygous mutant spinal cords (Fig. 3L). Consistent with the reduction in the floor plate and V3 interneurons, *Olig2*-expressing motor neuron progenitors, which were dorsal to V3 interneurons in the wild-type spinal cord (Fig. 3P), were closer to the ventral midline of the *Gli2*$^{\Delta CLRKIn/\Delta CLRKIn}$ homozygous mutant spinal cords (Fig. 3Q). Although our qRT-PCR and immunoblot analyses showed slightly less *Gli2*$^{\Delta CLR}$ mRNA and Gli2$^{\Delta CLR}$ protein in *Gli2*$^{\Delta CLRKI/\Delta CLRKI}$ than in *Gli2*$^{\Delta CLRKIn/\Delta CLRKIn}$ homozygous mutants, the *Gli2*$^{\Delta CLRKI}$ homozygous spinal cords exhibit the same degree of reduction in floor plate and V3 interneurons, as well as the ventral expansion of the motor neuron domain (Fig. 3H,M,R).

The defects in floor plate and V3 interneuron induction in the *Gli2*$^{\Delta CLRKIn/\Delta CLRKIn}$ and *Gli2*$^{\Delta CLRKI/\Delta CLRKI}$ homozygous mutant spinal cords were similar, but not as severe as the *Gli2*$^{-/-}$ mutant spinal cord, in which Foxa2 expression was largely absent (Fig. 3J) and Nkx2.2-expressing cells were greatly reduced in number (Fig. 3O), whereas Olig2 expression was expanded to the ventral midline (Fig. 3T; Ding et al., 1998; Matise et al., 1998). We reasoned that the difference might result from the higher than normal levels of the Gli2$^{\Delta CLR}$ protein in these mutants. To test this hypothesis, we examined the spinal cord development in *Gli2*$^{\Delta CLRKIn/-}$ and *Gli2*$^{\Delta CLRKI/-}$ transheterozygous mutants, in which the levels of Gli2$^{\Delta CLR}$ protein were more similar to that of Gli2 in wild-type embryos. Indeed, these *Gli2*$^{\Delta CLRKI/-}$ transheterozygous mutants exhibit smaller floor plate and V3 interneuron domains resembling those in *Gli2*$^{-/-}$ homozygous

Development (2015) 142, 1651-1660 doi:10.1242/dev.119669

mutants (Fig. 3I,N). Consequently, the motor neuron progenitor domain expands further into the ventral-most region of the spinal cord (Fig. 3S).

The ventral patterning defects in *Gli2*$^{\Delta CLRKIn/\Delta CLRKIn}$, *Gli2*$^{\Delta CLRKI/\Delta CLRKI}$ homozygous and *Gli2*$^{\Delta CLRKI/-}$ transheterozygous mutant spinal cords suggested that Hh signaling was compromised due to the failure in Gli2$^{\Delta CLR}$ activation. To determine the level of Hh pathway activation directly, we examined the expression of *Gli1*, a direct transcriptional target gene of Hh signaling. Through qRT-PCR, we found a progressive decrease in the expression level of *Gli1* in *Gli2*$^{\Delta CLRKIn/\Delta CLRKIn}$, *Gli2*$^{\Delta CLRKI/\Delta CLRKI}$ homozygous, *Gli2*$^{\Delta CLRKIn/-}$ transheterozygous and *Gli2*$^{-/-}$ mutant embryos, suggesting a reduction in Hh pathway activation (Fig. 3U). To better reveal *Gli1* expression in the developing embryos, we examined the expression of a *lacZ* reporter gene inserted in the *Gli1* locus (Bai et al., 2002). As reported, the *lacZ* expression nicely recapitulated the expression pattern of *Gli1* in the ventral CNS, posterior limb buds and the gut (Fig. 3V). In *Gli2*$^{\Delta CLRKI/\Delta CLRKI}$ homozygous mutant embryos, the reporter expression was greatly decreased, especially in the midbrain and anterior hindbrain regions (Fig. 3W). In summary, the *Gli2* null-like brain morphology, abnormal patterning of the ventral neural tube and reduced *Gli1* expression, suggest that Gli2$^{\Delta CLR}$ fails to activate Hh signaling efficiently in embryonic development.

The more severe disruption of Hh signaling in the transheterozygous mutants (*Gli2*$^{\Delta CLRKIn/-}$ and *Gli2*$^{\Delta CLRKI/-}$) than the homozygous mutants (*Gli2*$^{\Delta CLRKIn/\Delta CLRKIn}$ and *Gli2*$^{\Delta CLRKI/\Delta CLRKI}$) suggested that the levels of Gli2$^{\Delta CLR}$ protein in these mutants had a noticeable impact on Hh target gene activation. To minimize this impact, we used the transheterozygous mutants, in which the level of Gli2$^{\Delta CLR}$ protein was more similar to that of endogenous Gli2, in studies for the rest of this paper.

Gli2$^{\Delta CLRKI-}$*;Gli3*$^{-/-}$ double mutants resemble *Gli2*$^{-/-}$*;Gli3*$^{-/-}$ double mutants

Although *Gli2*$^{\Delta CLR}$ knock-in mutants resemble *Gli2*-null mutants, the presence of small numbers of *Foxa2*-expressing floor-plate cells in the spinal cords of these mutants suggested that Hh pathway was slightly more activated in *Gli2*$^{\Delta CLR}$ knock-in mutants than in *Gli2*-null mutants. One explanation for this minor difference is that the higher level of Gli2$^{\Delta CLR}$ protein may sequester negative regulators such as suppressor of fused (Sufu), lowering the threshold for Gli3 activator to activate Hh target genes. To test whether this is true, we removed *Gli3* from *Gli2*$^{\Delta CLRKI/-}$ mutants to obtain *Gli2*$^{\Delta CLRKI/-}$*;Gli3*$^{-/-}$ double mutants. At E9.5, these *Gli2*$^{\Delta CLRKI/-}$*;Gli3*$^{-/-}$ double mutants (Fig. 4B) exhibit exencephaly, like *Gli2*$^{-/-}$*;Gli3*$^{-/-}$ double mutants (Fig. 4C). The expression of *Foxa2* (Fig. 4E) and *Nkx2.2* (Fig. 4H) was absent in the *Gli2*$^{\Delta CLRKI/-}$*;Gli3*$^{-/-}$ double mutant spinal cord, similar to *Gli2*$^{-/-}$*;Gli3*$^{-/-}$ double mutants (Fig. 4F,I). *Olig2* and *Pax6*, which were excluded from the ventral-most region of the wild-type spinal cord (Fig. 4J,M), were expressed in the ventral spinal cord of both *Gli2*$^{\Delta CLRKI/-}$*;Gli3*$^{-/-}$ (Fig. 4K,N) and *Gli2*$^{-/-}$*;Gli3*$^{-/-}$ (Fig. 4L,O) double mutants. The identical morphological and spinal cord patterning defects in *Gli2*$^{\Delta CLRKI/-}$*;Gli3* and *Gli2*$^{-/-}$*;Gli3*$^{-/-}$ double mutants further suggests that Gli2$^{\Delta CLR}$ is incapable of transducing the Hh signal that is crucial for the neural tube development, and the Gli3 activator likely underlies the partial activation of Hh signaling in *Gli2*$^{\Delta CLR}$ knock-in mutants.

Activated Smo fails to activate Gli2$^{\Delta CLR}$

The Hh receptor Ptch1 and its downstream target Smo both localize to the primary cilium, and Smo activation is dependent on its ciliary localization (Corbit et al., 2005; Rohatgi et al., 2007). Local interactions

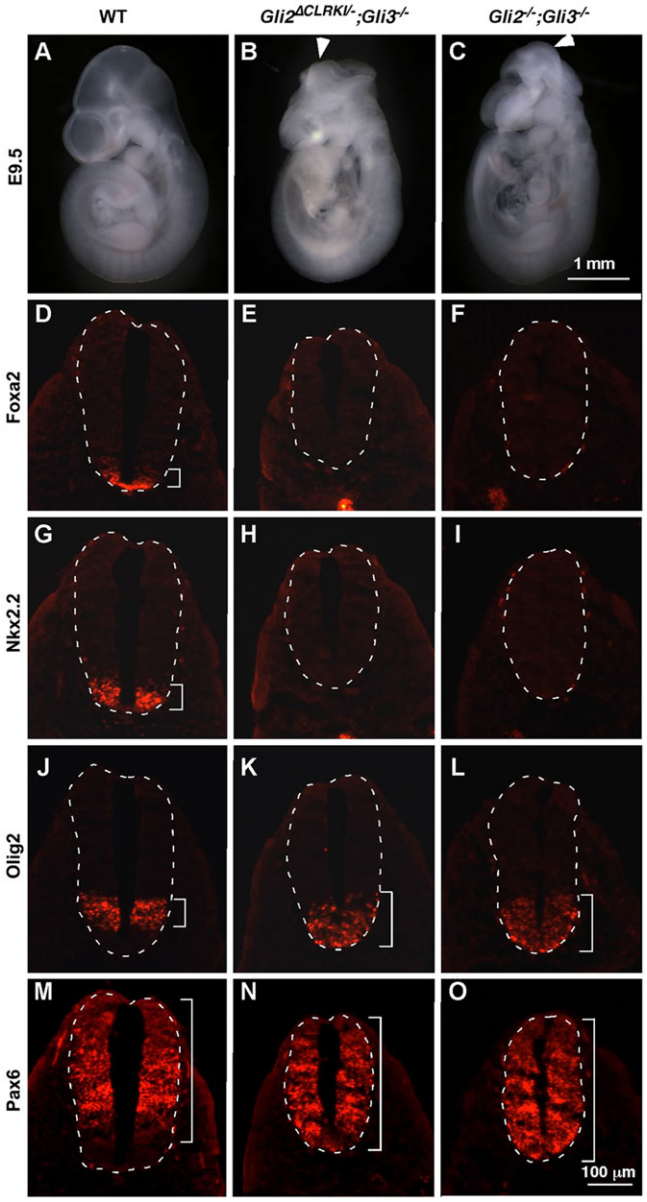

Fig. 4. Spinal cord patterning in *Gli2*$^{\Delta CLRKI}$*;Gli3* double mutants resembles that of *Gli2;Gli3* double mutants. (A-C) Lateral views of E9.5 embryos. Arrowheads indicate exencephaly in B,C. (D-O) Immunofluorescent images of transverse sections through the E9.5 spinal cords at the thoracic level. Similar patterns were observed in more posterior regions. Dashed lines outline the spinal cords. Brackets show the expression domains. (D-I) *Foxa2* and *Nkx2.2* are expressed in the ventral-most regions of the wild-type spinal cords (n=7; D,G), but are absent in the *Gli2*$^{\Delta CLRKI-}$*;Gli3*$^{-/-}$ (n=3; E,H) and *Gli2*$^{-/-}$*;Gli3*$^{-/-}$ (n=4; F,I) double mutant spinal cords. (J-O) *Olig2* and *Pax6* are excluded from the ventral-most regions of the wild type (J,M), but not of the *Gli2*$^{\Delta CLRKI-}$*;Gli3*$^{-/-}$ (K,N) and *Gli2*$^{-/-}$*;Gli3*$^{-/-}$ (L,O) double mutant spinal cords.

between Smo and a Ci (fly homolog of Gli2)-containing signaling complex mediate Hh signaling in *Drosophila* (Briscoe and Thérond, 2013). If local interaction between vertebrate Smo and Gli2 inside the cilium similarly underlies Gli2 activation by Smo, Smo activation would not result in the activation of the non-ciliary Gli2$^{\Delta CLR}$. To test this hypothesis, we treated the *Gli2*$^{\Delta CLRKIn/\Delta CLRKIn}$ mutant MEFs with SAG. The SAG treatment induced similar ciliary localization of Smo in wild-type, *Gli2*$^{-/-}$ and *Gli2*$^{\Delta CLRKIn/\Delta CLRKIn}$ mutant MEFs (data not shown). It also greatly increased the expression of Hh target gene *Gli1*

Development (2015) 142, 1651-1660 doi:10.1242/dev.119669

in wild-type MEFs (Fig. 5A). By contrast, the expression of *Gli1* was only slightly increased in *Gli2*$^{-/-}$ and *Gli2*$^{\Delta CLRKIn/\Delta CLRKIn}$ mutant MEFs, suggesting a disruption of the signal transduction from Smo to Gli2$^{\Delta CLR}$ (Fig. 5A).

To determine whether Smo activation resulted in the activation of Gli2$^{\Delta CLR}$ *in vivo*, we examined the morphology, Hh target gene expression and spinal cord patterning in *Gli2*$^{\Delta CLRKI/-}$;*Ptch1*$^{-/-}$ double mutants. At E9.5, *Ptch1*$^{-/-}$ mutant embryos failed to turn and exhibited severe neural tube defects (Fig. 5B; Goodrich et al., 1997). The turning and neural tube defects were partially rescued in *Gli2*$^{\Delta CLRKI/-}$;*Ptch1*$^{-/-}$ and *Gli2*$^{-/-}$;*Ptch1*$^{-/-}$ double mutants, and some double mutants were noticeably larger than *Ptch1*$^{-/-}$ mutants (Fig. 5B). Hh target gene *Gli1* was expressed in a ventral-to-dorsal gradient in the E9.5 wild-type spinal cord (Fig. 5C). However, as reported previously, *Gli1* expression in the floor plate, the ventral-most part of the spinal cord, was downregulated by prolonged exposure to extremely high levels of Shh through a feedback mechanism (Ribes et al., 2010). *Gli1* expression was downregulated in the entire *Ptch1* mutant spinal cord, consistent with very high levels of Hh pathway activation (Fig. 5C). In *Gli2*$^{\Delta CLRKI/-}$;*Ptch1*$^{-/-}$ double mutants, *Gli1* expression was restored in the dorsal spinal cord, suggesting that Hh pathway activation was less than that in *Ptch1* mutants (Fig. 5C). Interestingly, the expression pattern of *Gli1* in the *Gli2*$^{\Delta CLRKI/-}$;*Ptch1*$^{-/-}$ double mutant spinal cord was similar to that in *Gli2*$^{\Delta CLRKI/-}$;*Ptch1*$^{-/-}$ double mutants (Fig. 5C), suggesting that the reduction of Hh pathway activation in these mutants resulted from a disruption of Gli2$^{\Delta CLR}$ activation.

Consistent with the extreme activation of Hh signaling, *Foxa2*- and *Nkx2.2*-expressing cells spread throughout the *Ptch1*$^{-/-}$ mutant spinal cord (Fig. 5D). The expression of *Pax6* and *Olig2* was absent or restricted to few cells in the dorsal-most part of the spinal cord (Fig. 5D). Interestingly, both *Foxa2*- and *Nkx2.2*-expressing cells were restricted to the ventral regions of the *Gli2*$^{\Delta CLRKI/-}$;*Ptch1*$^{-/-}$ double mutant spinal cords, suggesting that Hh pathway activation in these mutants was insufficient to support the expression of these two genes in the dorsal spinal cord (Fig. 5D). Consistent with a reduction of Hh pathway activation, *Olig2* and *Pax6* expression was restored in the dorsal two-thirds of the *Gli2*$^{\Delta CLRKI/-}$;*Ptch1*$^{-/-}$ double mutant spinal cord (Fig. 5D). These changes in spinal cord patterning in *Gli2*$^{\Delta CLRKI/-}$;*Ptch1*$^{-/-}$ double mutants were similar to those in *Gli2*$^{-/-}$;*Ptch1*$^{-/-}$ double mutants (Fig. 5D), providing further support for the inability of Gli2$^{\Delta CLR}$ to respond to upstream Hh pathway activation *in vivo*.

Gli2$^{\Delta CLR}$ is active in the absence of Sufu

The results described thus far indicate that Gli2$^{\Delta CLR}$ does not respond to Hh pathway activation at the levels of Ptch1 or Smo. The parsimonious explanation for this phenomenon is that a local interaction at the cilium cannot be established between activated Smo and Gli2$^{\Delta CLR}$. Alternatively, the deletion of CLR may result in damage to the intrinsic transcriptional activity of Gli2 that failed to be detected in our *in vitro* overexpression analysis. To distinguish these two possibilities, we investigated whether Gli2$^{\Delta CLR}$ can be activated in the absence of Sufu, the inhibitory action of which on

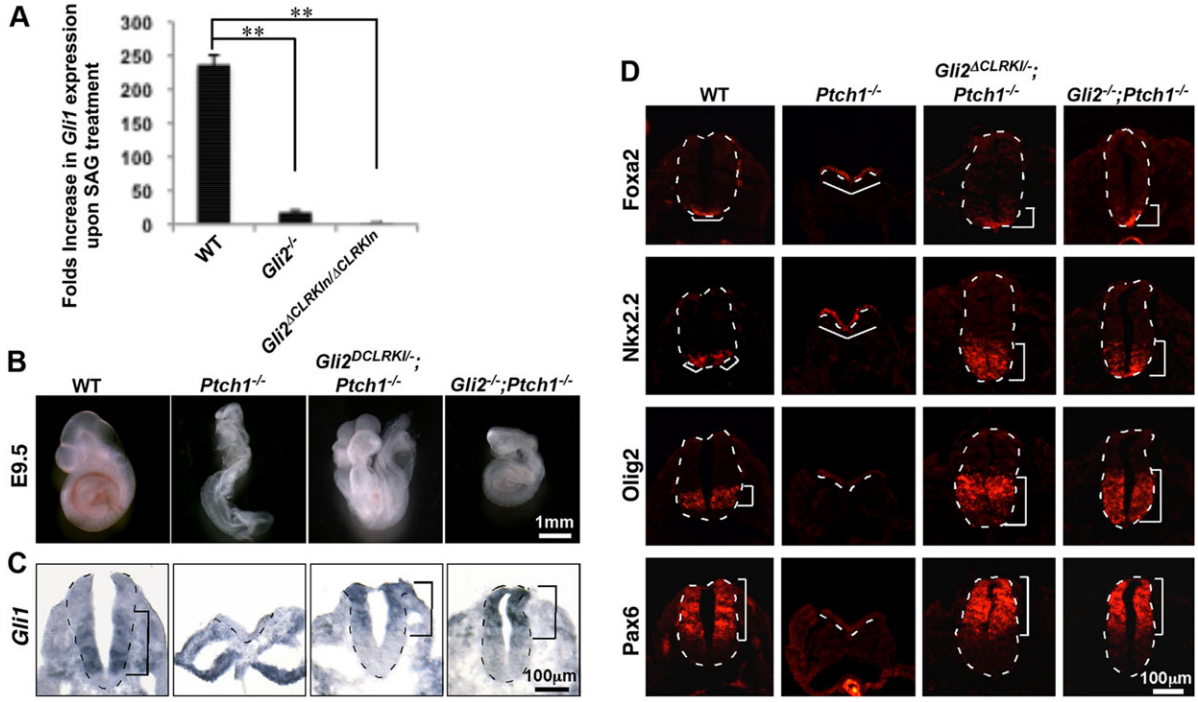

Fig. 5. Hh signaling fails to activate Gli2$^{\Delta CLR}$ *in vitro* and *in vivo*. (A) Activation of Smo with SAG greatly increases *Gli1* transcription in wild type, but not in *Gli2*$^{-/-}$ or *Gli2*$^{\Delta CLRKIn/\Delta CLRKIn}$ mutant MEFs. *n*=3 independent experiments. ***P*<0.01, unpaired Student's *t*-test. (B) Lateral views of E9.5 embryos. The *Gli2*$^{\Delta CLRKI/-}$;*Ptch1*$^{-/-}$ double mutant is larger than the *Ptch1*$^{-/-}$ mutant, and the *Gli2*$^{-/-}$;*Ptch1*$^{-/-}$ mutant has completed turning. (C) RNA *in situ* hybridization images of transverse sections through the E9.5 spinal cords. *Gli1* expression was inhibited by the high level of Hh signaling in the *Ptch1*$^{-/-}$ mutant spinal cord (*n*=4), but was present in the dorsal half of the *Gli2*$^{\Delta CLRKI/-}$;*Ptch1*$^{-/-}$ (*n*=4) and *Gli2*$^{-/-}$;*Ptch1*$^{-/-}$ (*n*=4) double mutant spinal cords. Dashed lines outline the spinal cords. Brackets show the expression domains. (D) Immunofluorescent images of transverse sections through the E9.5 spinal cords at the thoracic level. Similar patterns were observed in more posterior regions. *Foxa2* and *Nkx2.2* are expressed throughout the spinal cord, whereas *Olig2* and *Pax6* expression is absent in *Ptch1* mutants (*n*=3). By contrast, *Foxa2*, *Nkx2.2* and *Olig2* expression is restricted to the ventral parts of the *Gli2*$^{\Delta CLRKI/-}$;*Ptch1*$^{-/-}$ (*n*=3) and *Gli2*$^{-/-}$;*Ptch1*$^{-/-}$ (*n*=2) double mutant spinal cords. *Pax6* expression is also restored in the *Gli2*$^{\Delta CLRKI/-}$;*Ptch1*$^{-/-}$ and *Gli2*$^{-/-}$;*Ptch1*$^{-/-}$ mutant spinal cords. Dashed lines outline the spinal cords. Brackets show the expression domains.

Development (2015) 142, 1651-1660 doi:10.1242/dev.119669

Gli2 can be relieved only through a cilium-dependent process under physiological condition (Kim et al., 2009).

As reported previously, *Sufu*$^{-/-}$ mutants failed to turn and exhibited severe neural tube defects (Fig. 6A; Cooper et al., 2005; Svärd et al., 2006). There was no obvious rescue of these defects in *Gli2*$^{\Delta CLRKI/-}$*;Sufu*$^{-/-}$ double mutants (Fig. 6A). The expression of Hh target gene *Gli1* was restricted to the dorsal spinal cords of both *Sufu*$^{-/-}$ mutants and *Gli2*$^{\Delta CLRKI/-}$*; Sufu*$^{-/-}$ double mutants (Fig. 6B), suggesting that Gli2$^{\Delta CLR}$ is capable of activating target gene expression in the absence of *Sufu*. Furthermore, these results also suggest that the disruption of Gli2$^{\Delta CLR}$ activation in *Gli2*$^{\Delta CLR}$ knock-in mutants results from failure to release Gli2$^{\Delta CLR}$ from Sufu inhibition.

Consistent with the widespread activation of Hh signaling, *Foxa2* and *Nkx2.2* expression domains greatly expanded in the E9.5 *Sufu*$^{-/-}$ mutant spinal cord (Fig. 6C). Meanwhile, the expression domains of *Olig2* and *Pax6* were shifted dorsally in the *Sufu*$^{-/-}$ mutant spinal cord (Fig. 6C). We have recently shown that removing *Gli2* from *Sufu* mutants, as in *Gli2*$^{-/-}$*;Sufu*$^{-/-}$ double mutants, led to the absence of *Foxa2* and *Nkx2.2* expression, along with ventral expansion of the *Olig2* and *Pax6* expression, suggesting that Gli2 was the primary activator of Hh signaling in the absence of *Sufu* (Liu et al., 2012). In striking contrast to the absence of *Foxa2* and *Nkx2.2* expression in *Gli2*$^{-/-}$*;Sufu*$^{-/-}$ double mutants, these two genes were expressed in most cells of the *Gli2*$^{\Delta CLRKI/-}$*;Sufu*$^{-/-}$ double mutant spinal cord, similar to that of *Sufu*$^{-/-}$ mutants (Fig. 6C). In addition, *Olig2* and *Pax6* expression remained dorsally restricted in the *Gli2*$^{\Delta CLRKI/-}$*;Sufu*$^{-/-}$ double mutant spinal cord, as seen in *Sufu*$^{-/-}$ mutants (Fig. 6C). The similarity between *Sufu*$^{-/-}$ mutant and *Gli2*$^{\Delta CLRKI/-}$*;Sufu*$^{-/-}$ double mutant spinal cord patterning suggests that Gli2$^{\Delta CLR}$ retains its intrinsic transcriptional activity that can be released by the removal of Sufu.

We and others have previously shown that the protein levels of Gli2 and Gli3 decrease in *Sufu*$^{-/-}$ embryos, possibly due to Cullin3/Spop (speckle type POZ protein)-mediated proteasomal degradation (Chen et al., 2009; Jia et al., 2009; Wang et al., 2010). To determine whether Gli2$^{\Delta CLR}$ is under the same regulation, we performed immunoblot analyses on E9.5 whole-embryo lysates. Interestingly, although the level of Gli2$^{\Delta CLR}$ in *Gli2*$^{\Delta CLRKI/-}$ mutant embryos was approximately fourfold higher than Gli2 in wild-type embryos, it was decreased drastically in *Gli2*$^{\Delta CLRKI/-}$*;Sufu*$^{-/-}$ double mutants such that it was comparable with that of Gli2 in *Sufu*$^{-/-}$ mutants (Fig. 6D). Therefore, the widespread activation of Hh signaling in *Gli2*$^{\Delta CLRKI/-}$*;Sufu*$^{-/-}$ results from its uncompromised intrinsic transcriptional activity, rather than from an artifact of high protein level.

DISCUSSION

An essential role for the primary cilium in Hh pathway and Gli protein activation has been well established by numerous genetic studies in various vertebrate species in the past decade (Nozawa et al., 2013). However, the role of the ciliary localization of Gli

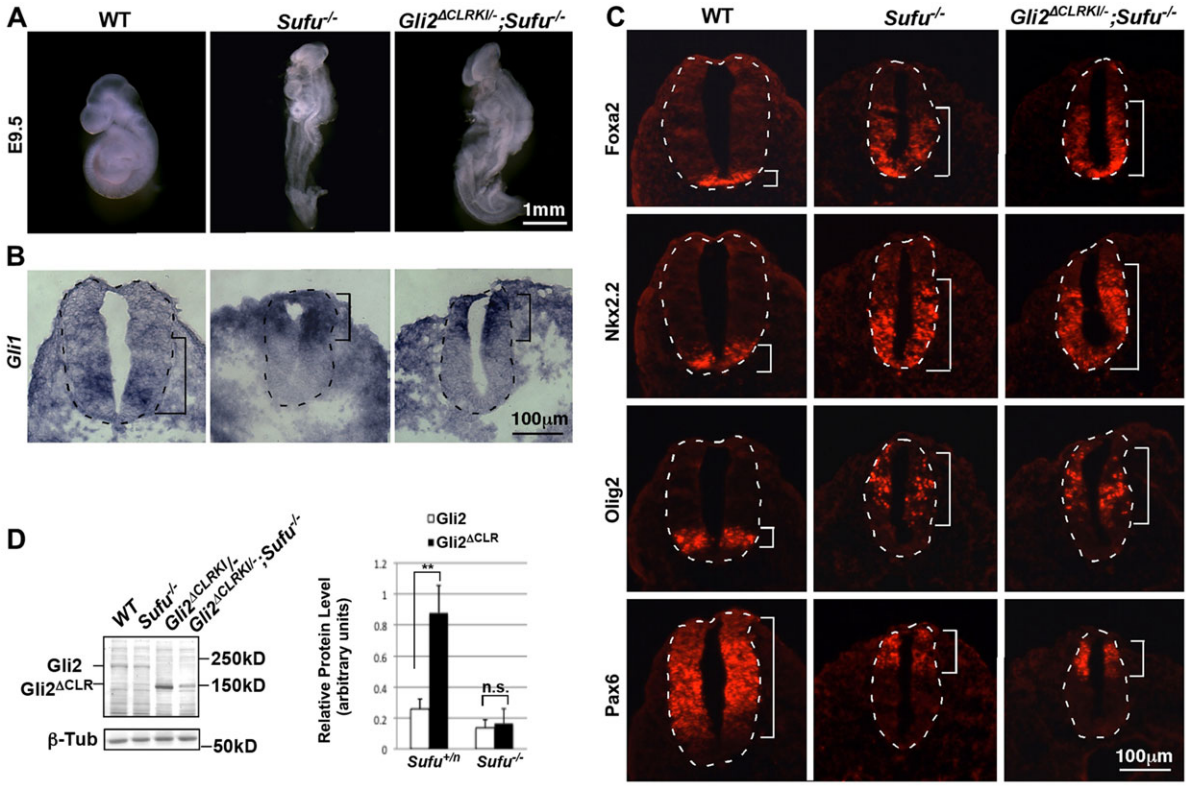

Fig. 6. The intrinsic transcriptional activator activity was not disrupted in Gli2$^{\Delta CLR}$. (A) Lateral views of E9.5 embryos showing similar exencephaly and turning defects in *Sufu*$^{-/-}$ and *Gli2*$^{\Delta CLRKII-}$*;Sufu*$^{-/-}$ double mutants. (B) Transverse sections of E9.5 embryos processed for RNA *in situ* hybridization. The expression of Hh target gene *Gli1* is dorsally restricted in *Sufu*$^{-/-}$ (n=3) and *Gli2*$^{\Delta CLRKII-}$*;Sufu*$^{-/-}$ double mutant (n=4) spinal cords. (C) Transverse sections of E9.5 embryos processed for immunofluorescent analysis. Shown are sections at the thoracic level. Similar patterns were observed in more posterior regions. The expression domains of *Foxa2* and *Nkx2.2* are expanded into the dorsal spinal cords of *Sufu*$^{-/-}$mutant (n=4) and *Gli2*$^{\Delta CLRKII-}$*;Sufu*$^{-/-}$ double mutant (n=4) spinal cords. *Olig2* expression is shifted dorsally in *Sufu*$^{-/-}$ mutant and *Gli2*$^{\Delta CLRKII-}$*;Sufu*$^{-/-}$ double mutant spinal cords. *Pax6* expression is restricted to the dorsal-most part of *Sufu*$^{-/-}$ mutant and *Gli2*$^{\Delta CLRKII-}$*;Sufu*$^{-/-}$ double mutant spinal cords. (D) Immunoblot analysis shows decrease in both Gli2 and Gli2$^{\Delta CLR}$ protein levels in the absence of Sufu. **P<0.01, n.s., P>0.05, unpaired Student's t-test.

Development (2015) 142, 1651-1660 doi:10.1242/dev.119669

proteins in their activation has not yet been determined. One commonly taken approach to address this issue has been to disrupt the cellular and/or ciliary transport machinery. In one such study, the disruption of the cytoplasmic microtubule network through a drug treatment abolished the ciliary localization of Gli2 and disrupted the Hh signaling (Kim et al., 2009). Similarly, mutations in a microtubule motor protein Kif7, or in an intraflagellar transport protein Ift25, affected Gli2 ciliary localization and Hh pathway activation (Cheung et al., 2009; Endoh-Yamagami et al., 2009; He et al., 2014; Keady et al., 2012; Liem et al., 2009). One major concern with this approach is that additional proteins and processes affected by the disruption of cytoskeleton or transport machinery may contribute to the observed disruption of Hh signaling. Moreover, the Gli ciliary localization was only partially affected by many of these mutations, further complicating the interpretation of the results.

A more-targeted approach to study the role of the ciliary localization of Gli2 in its activation is to determine whether a non-ciliary variant of Gli2 can be activated by Hh signaling. It is crucial, however, to distinguish between the inability to respond to Hh pathway activation and the damage to the intrinsic transcriptional activity of the non-ciliary variant of Gli2. For example, a recent study found that the ciliary localization of a Gli2 variant lacking residues 852-1183 was greatly compromised compared with the full-length Gli2 (Santos and Reiter, 2014). However, this Gli2 variant acted as a transcriptional repressor when it was overexpressed, suggesting that the deletion has damaged its intrinsic transcriptional activator activity. Therefore, it could not be used to properly investigate the roles of the ciliary localization of Gli2 in its activation by Hh signaling.

In the current study, we address the relationship between Gli2 ciliary localization and activation using Gli2$^{\Delta CLR}$, a non-ciliary variant of Gli2. Through the study of *Gli2*$^{\Delta CLR}$ knock-in mutant cells and embryos, we show that Gli2$^{\Delta CLR}$ fails to respond to Hh pathway activation at the levels of Ptch1 or Smo. To rule out the possibility that the intrinsic transcriptional activity of Gli2 is disrupted in Gli2$^{\Delta CLR}$, we first show that its overexpression is sufficient to activate a Gli-responsive reporter expression in cultured cells. In addition, we show that Gli2$^{\Delta CLR}$ can support the same level of Hh pathway activation as endogenous Gli2 in the absence of Sufu. Therefore, the lack of Gli2$^{\Delta CLR}$ activation in *Gli2*$^{\Delta CLR}$ knock-in mutant embryos likely results from the failure in cilium-dependent relief of the inhibitory action of Sufu, not the disruption of intrinsic transcriptional activity of Gli2.

The simultaneous loss of ciliary localization of Gli2$^{\Delta CLR}$ and the failure in the relief of the inhibitory action of Sufu on this non-ciliary variant of Gli2 strongly suggest that the ciliary localization of Gli2 is crucial for the Hh-dependent activation of this protein. However, we cannot formally rule out the possibility that the CLR may also be important for potential conformational changes of Gli2 that allow its dissociation from Sufu, which could be independent of the loss of Gli2 ciliary localization. To formally establish the causative relationship between the ciliary localization and activation of Gli2, it would be ideal to investigate whether restoring the ciliary localization of Gli2$^{\Delta CLR}$ with an unrelated ciliary-localization motif would allow normal Hh signaling. However, this could prove to be difficult because Gli2 appears to dynamically traffic through a special ciliary tip compartment, thus simply directing Gli2$^{\Delta CLR}$ localization to the cilium may not be sufficient to restore its response to Hh signaling (He et al., 2014).

Previous studies have shown that cilium-dependent regulation of Hh signaling was dependent on the proper levels of Gli proteins (Chen et al., 2009; Jia et al., 2009). Overexpression of Gli1 or Gli2 bypasses the inhibitory regulation of Sufu, thus activating the Hh pathway independently of the cilium. Therefore, we were concerned about the approximately fourfold difference between the Gli2$^{\Delta CLR}$ protein level in *Gli2*$^{\Delta CLRKI/-}$ transheterozygous mutant embryos and the Gli2 protein level in wild type. Interestingly, despite the increase in Gli2$^{\Delta CLR}$ protein levels, we observed decreased Hh signaling in *Gli2*$^{\Delta CLRKI/-}$ transheterozygous mutants. This suggests that Sufu is likely present in large excess compared with Gli proteins, as previously reported in fruit flies (Farzan et al., 2009). In effect, this increase in Gli2$^{\Delta CLR}$ protein levels helps to clarify that it is the lack of activation, rather than insufficient amount of protein, that underlies the Hh signaling defects in *Gli2*$^{\Delta CLRKI}$ mutants.

cAMP-dependent protein kinase (PKA) plays an essential negative role in Hh signaling (Tuson et al., 2011). A recent study showed that overexpressing a Gli2 variant lacking six PKA sites highly activates Hh pathway in cultured cells and chicken spinal cords (Niewiadomski et al., 2014). The non-ciliary Gli2$^{\Delta CLR}$ variant we studied here also lacks all six PKA sites, and yet it fails to activate Hh pathway in *Gli2*$^{\Delta CLRKI}$ mutant embryos. It was recently reported that Hh pathway activation in the absence of PKA remained cilium dependent (Tuson et al., 2011). Therefore, it is likely that even a PKA-insensitive Gli2 variant requires ciliary localization to be activated. Again, it is worth noting that the activity of any Gli2 variant has to be determined in a system in which the level of the Gli2 variant is not high enough to override the intricate regulatory mechanisms involving the cilium and Sufu, as we have demonstrated here and in previous studies (Chen et al., 2009; Jia et al., 2009).

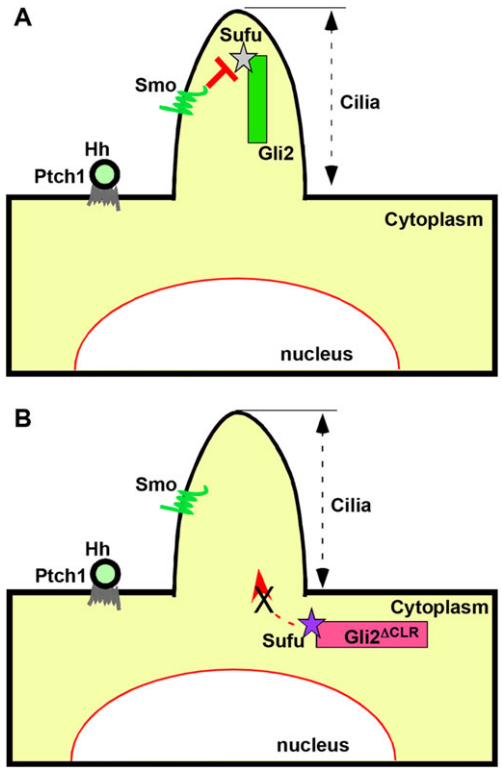

Fig. 7. The ciliary localization of Gli2 is essential for its activation. (A) In wild-type cells, activated Smo interacts with Gli2 and Sufu inside the cilium, releasing Gli2 from Sufu inhibition. (B) In *Gli2*$^{\Delta CLR}$ knock-in mutant cells, Gli2$^{\Delta CLR}$ fails to enter the cilium to interact with activated Smo, and remains inhibited by Sufu.

Development (2015) 142, 1651-1660 doi:10.1242/dev.119669

It is surprising that Gli2$^{\Delta CLR}$ exhibits higher intrinsic transcriptional activity than Gli2 in our luciferase reporter assay, despite its predominant cytoplasmic localization. It is possible that the removal of inhibitory post-translational modification may underlie this increase in transcriptional activity. For example, the acetylation of K518 in Gli1 has been shown to inhibit its transcriptional activity (Canettieri et al., 2010). The corresponding lysine in Gli2, K740, was removed in Gli2$^{\Delta CLR}$, which could contribute to the increase in its intrinsic transcriptional activity.

In summary, we show here that Hh signaling fails to activate a non-ciliary Gli2$^{\Delta CLR}$ variant *in vivo* by relieving the inhibitory actions of Sufu. Based on our results, we propose that the ciliary localization of Gli2 allows its activation, likely through local interaction with activated Smo that relieves Gli2 from its inhibitor Sufu (Fig. 7A). However, Gli2$^{\Delta CLR}$ is under constitutive inhibition by Sufu because it fails to travel to the cilium to interact with activated Smo (Fig. 7B). An exciting future direction would be to reveal the molecular events that directly lead to the activation of Gli2 once it is inside the cilium.

MATERIALS AND METHODS

Tissue culture, transfection and immunofluorescence

Mouse embryonic fibroblasts were prepared from E11.5 embryos as previously described (Jia et al., 2009). Cells were transfected with Lipofectamine 2000 (Life Technologies), JetPrime (Polyplus-Transfection) or PEI (Polysciences) according to the manufacturer's recommendations. Immunofluorescence analyses were carried out as previously reported (Zeng et al., 2010b). Antibodies used were acetylated α-tubulin (Sigma-Aldrich, T7451, 1:1000), GFP (Life Technologies, A11122, 1:1000) and Gli2 (R&D Systems, AF3635, 1:500, raised against the N-terminal 416 amino acids of mouse Gli2).

Quantitative RT-PCR

RNA was extracted from embryos or cultured cells using a NucleoSpin RNA miniprep kit (Macherey-Nagel). cDNA was synthesized using qScript cDNA SuperMix (Quanta Biosciences). PCR reactions were performed using a StepOnePlus Real-time PCR system (Applied Biosystems). All samples were analyzed in triplicate and normalized to the housekeeping gene *Gapdh*. Primers used for qRT-PCR were: Gli2(1067)F, 5′-GACCTAC-AACGCATGATTCGG-3′ and Gli2(1117)R, 5′-GATGTAAGCTACCAG-CGAGTTGG-3′; Gli1(1081)F, 5′-CGTTTGAAGGCTGTCGGAAG-3′ and Gli1(1131)R 5′-GCGTCTTGAGGTTTTCAAGGC-3′. The specificity of the primers was tested on null mutant embryos lacking target gene transcription and on cells overexpressing GFP-tagged target genes.

Luciferase reporter assay

Shh-L2 cells (a gift from Dr L. Lum, UT Southwestern Medical Center, Dallas, TX, USA) in 24-well plates were transfected with *GFP-Gli2*, *GFP-Gli2*$^{\Delta CLR}$, or control empty *GFP* vector, alone or together with Sufu. Luciferase assays were performed 24 h after transfection using a dual-luciferase reporter assay system (Promega). Luminescence was measured in a Turner Biosystems 20/20n luminometer. Firefly luciferase activities were normalized to those of Renilla luciferase.

Immunoblot analyses

Whole-cell protein lysates were prepared, separated on SDS polyacrylamide gel and transferred to nitrocellulose membrane according to a previously described protocol (Zeng et al., 2010b). After primary antibody incubation, membranes were incubated with IRD680- and IRD800-conjugated secondary antibodies (LI-COR), and scanned on a LI-COR Odyssey CLx imaging system. Quantitative analysis was performed using Image Studio (LI-COR). Primary antibodies used were GFP (Life Technologies, A11122, 1:10,000), Gli2 (R&D Systems, AF3635, 1:1000) and β-tubulin (Sigma-Aldrich, T5201, 1:10,000).

Animals

E14 mouse embryonic stem (ES) cells (MMRRC) were transfected with linearized *Gli2*$^{\Delta CLRKIn}$ targeting construct using a BioRad GenePulsor electroporation system as described previously (Zeng et al., 2010a). Genomic DNAs from G418-resistant ES cell clones were cut with *Asp*718 (Roche) and screened through Southern blot analyses using a 5′ external probe. Genomic DNAs from the targeted clones were cut with *Bam*HI and screened again through Southern blot using a 3′ external probe. The homologous recombination events were further confirmed with PCR using locus-specific primers. Two targeted *Gli2*$^{\Delta CLRKIn}$ ES cell clones were injected into C57/BL6 blastocysts (Charles River Labs). The resulting male chimeras and their male descendants were bred to wild-type 129 or C3H females (Charles River Labs). The genotypes of *Gli2*$^{\Delta CLRKIn}$ and *Gli2*$^{\Delta CLRKI}$ mice and embryos were determined with PCR using previously described primers (Bai and Joyner, 2001).

Other mutant mouse strains used in this study include *Gli1*^{tm2Alj} (Bai et al., 2002), *Gli2*$^{tm2.1Alj}$ (Bai and Joyner, 2001), *Gli3*$^{Xt\text{-}J}$ (Büscher et al., 1998), *Ptch1*^{tm1Mps} (Goodrich et al., 1997) and *Sufu*^{tm1Rto} (Svärd et al., 2006), and were genotyped as described. The use of the animals in this work was approved by the IACUC at the Penn State University (PA, USA).

Immunohistochemistry and RNA *in situ* hybridization

Immunohistochemistry using Cy3-labeled secondary antibodies as well as RNA *in situ* hybridization using DIG-labeled RNA probes were described by Liu et al. (2012). Antibodies used were Foxa2 (DHSB, 1:40), Nk2.2 (DHSB, 1:20), Pax6 (DSHB, 1:500) and Olig2 (Millipore, AB9610, 1:1000).

Acknowledgements

We thank Drs Yingwei Mao and Douglas Cavener for critically reading the manuscript. We thank Drs A. Joyner, L. Lum, M. Scott and R. Toftgard for sharing reagents. We also thank Dr Yijia Gu for his help with the statistical analysis. The monoclonal antibodies against Foxa2, Nkx2.2 and Pax6 developed by Drs Jessell and Kawakami were obtained from the Developmental Studies Hybridoma Bank developed under the auspices of the NICHD and maintained by The University of Iowa, Department of Biological Sciences, Iowa City, IA 52242, USA.

Competing interests

The authors declare no competing or financial interests.

Author contributions

A.L. designed the experiments. J.L. and H.Z. performed the experiments. J.L., H.Z. and A.L. analyzed the data and wrote the manuscript.

Funding

This work was funded by National Science Foundation grants [IOS-0949877 and IOS-1257540].

Supplementary material

Supplementary material available online at
http://dev.biologists.org/lookup/suppl/doi:10.1242/dev.119669/-/DC1

References

Bai, C. B. and Joyner, A. L. (2001). Gli1 can rescue the in vivo function of Gli2. *Development* **128**, 5161-5172.

Bai, C. B., Auerbach, W., Lee, J. S., Stephen, D. and Joyner, A. L. (2002). Gli2, but not Gli1, is required for initial Shh signaling and ectopic activation of the Shh pathway. *Development* **129**, 4753-4761.

Bai, C. B., Stephen, D. and Joyner, A. L. (2004). All mouse ventral spinal cord patterning by hedgehog is Gli dependent and involves an activator function of Gli3. *Dev. Cell* **6**, 103-115.

Briscoe, J. and Thérond, P. P. (2013). The mechanisms of Hedgehog signalling and its roles in development and disease. *Nat. Rev. Mol. Cell Biol.* **14**, 418-431.

Büscher, D., Grotewold, L. and Rüther, U. (1998). The Xt^{J} allele generates a Gli3 fusion transcript. *Mamm. Genome* **9**, 676-678.

Canettieri, G., Di Marcotullio, L., Greco, A., Coni, S., Antonucci, L., Infante, P., Pietrosanti, L., De Smaele, E., Ferretti, E., Miele, E. et al. (2010). Histone deacetylase and Cullin3-REN^{KCTD11} ubiquitin ligase interplay regulates Hedgehog signalling through Gli acetylation. *Nat. Cell Biol.* **12**, 132-142.

Chen, M.-H., Wilson, C. W., Li, Y.-J., Law, K. K. L., Lu, C.-S., Gacayan, R., Zhang, X., Hui, C.-c. and Chuang, P.-T. (2009). Cilium-independent regulation of Gli protein

Development (2015) 142, 1651-1660 doi:10.1242/dev.119669

function by Sufu in Hedgehog signaling is evolutionarily conserved. *Genes Dev.* **23**, 1910-1928.

Cheung, H. O.-L., Zhang, X., Ribeiro, A., Mo, R., Makino, S., Puviindran, V., Law, K. K. L., Briscoe, J. and Hui, C.-c. (2009). The kinesin protein Kif7 is a critical regulator of Gli transcription factors in mammalian hedgehog signaling. *Sci. Signal.* **2**, ra29.

Cooper, A. F., Yu, K. P., Brueckner, M., Brailey, L. L., Johnson, L., McGrath, J. M. and Bale, A. E. (2005). Cardiac and CNS defects in a mouse with targeted disruption of suppressor of fused. *Development* **132**, 4407-4417.

Corbit, K. C., Aanstad, P., Singla, V., Norman, A. R., Stainier, D. Y. R. and Reiter, J. F. (2005). Vertebrate Smoothened functions at the primary cilium. *Nature* **437**, 1018-1021.

Ding, Q., Motoyama, J., Gasca, S., Mo, R., Sasaki, H., Rossant, J. and Hui, C. C. (1998). Diminished Sonic hedgehog signaling and lack of floor plate differentiation in Gli2 mutant mice. *Development* **125**, 2533-2543.

Endoh-Yamagami, S., Evangelista, M., Wilson, D., Wen, X., Theunissen, J.-W., Phamluong, K., Davis, M., Scales, S. J., Solloway, M. J., de Sauvage, F. J. et al. (2009). The mammalian Cos2 homolog Kif7 plays an essential role in modulating Hh signal transduction during development. *Curr. Biol.* **19**, 1320-1326.

Farzan, S. F., Stegman, M. A., Ogden, S. K., Ascano, M., Jr, Black, K. E., Tacchelly, O. and Robbins, D. J. (2009). A quantification of pathway components supports a novel model of Hedgehog signal transduction. *J. Biol. Chem.* **284**, 28874-28884.

Goetz, S. C. and Anderson, K. V. (2010). The primary cilium: a signalling centre during vertebrate development. *Nat. Rev. Genet.* **11**, 331-344.

Goodrich, L. V., Milenković, L., Higgins, K. M. and Scott, M. P. (1997). Altered neural cell fates and medulloblastoma in mouse patched mutants. *Science* **277**, 1109-1113.

Haycraft, C. J., Banizs, B., Aydin-Son, Y., Zhang, Q., Michaud, E. J. and Yoder, B. K. (2005). Gli2 and Gli3 localize to cilia and require the intraflagellar transport protein polaris for processing and function. *PLoS Genet.* **1**, e53.

He, M., Subramanian, R., Bangs, F., Omelchenko, T., Liem, K. F., Jr, Kapoor, T. M. and Anderson, K. V. (2014). The kinesin-4 protein Kif7 regulates mammalian Hedgehog signalling by organizing the cilium tip compartment. *Nat. Cell Biol.* **16**, 663-672.

Humke, E. W., Dorn, K. V., Milenkovic, L., Scott, M. P. and Rohatgi, R. (2010). The output of Hedgehog signaling is controlled by the dynamic association between Suppressor of Fused and the Gli proteins. *Genes Dev.* **24**, 670-682.

Jia, J., Kolterud, A., Zeng, H., Hoover, A., Teglund, S., Toftgård, R. and Liu, A. (2009). Suppressor of Fused inhibits mammalian Hedgehog signaling in the absence of cilia. *Dev. Biol.* **330**, 452-460.

Keady, B. T., Samtani, R., Tobita, K., Tsuchya, M., San Agustin, J. T., Follit, J. A., Jonassen, J. A., Subramanian, R., Lo, C. W. and Pazour, G. J. (2012). IFT25 links the signal-dependent movement of Hedgehog components to intraflagellar transport. *Dev. Cell* **22**, 940-951.

Kim, J., Kato, M. and Beachy, P. A. (2009). Gli2 trafficking links Hedgehog-dependent activation of Smoothened in the primary cilium to transcriptional activation in the nucleus. *Proc. Natl. Acad. Sci. USA* **106**, 21666-21671.

Liem, K. F., Jr, He, M., Ocbina, P. J. R. and Anderson, K. V. (2009). Mouse Kif7/Costal2 is a cilia-associated protein that regulates Sonic hedgehog signaling. *Proc. Natl. Acad. Sci. USA* **106**, 13377-13382.

Lin, C., Yao, E., Wang, K., Nozawa, Y., Shimizu, H., Johnson, J. R., Chen, J.-N., Krogan, N. J. and Chuang, P.-T. (2014). Regulation of Sufu activity by p66beta and Mycbp provides new insight into vertebrate Hedgehog signaling. *Genes Dev.* **28**, 2547-2563.

Liu, J., Heydeck, W., Zeng, H. and Liu, A. (2012). Dual function of suppressor of fused in Hh pathway activation and mouse spinal cord patterning. *Dev. Biol.* **362**, 141-153.

Matise, M. P., Epstein, D. J., Park, H. L., Platt, K. A. and Joyner, A. L. (1998). Gli2 is required for induction of floor plate and adjacent cells, but not most ventral neurons in the mouse central nervous system. *Development* **125**, 2759-2770.

Niewiadomski, P., Kong, J. H., Ahrends, R., Ma, Y., Humke, E. W., Khan, S., Teruel, M. N., Novitch, B. G. and Rohatgi, R. (2014). Gli protein activity is controlled by multisite phosphorylation in vertebrate hedgehog signaling. *Cell Rep.* **6**, 168-181.

Nozawa, Y. I., Lin, C. and Chuang, P.-T. (2013). Hedgehog signaling from the primary cilium to the nucleus: an emerging picture of ciliary localization, trafficking and transduction. *Curr. Opin. Genet. Dev.* **23**, 429-437.

Pan, Y., Bai, C. B., Joyner, A. L. and Wang, B. (2006). Sonic hedgehog signaling regulates Gli2 transcriptional activity by suppressing its processing and degradation. *Mol. Cell. Biol.* **26**, 3365-3377.

Ribes, V., Balaskas, N., Sasai, N., Cruz, C., Dessaud, E., Cayuso, J., Tozer, S., Yang, L. L., Novitch, B., Marti, E. et al. (2010). Distinct Sonic Hedgehog signaling dynamics specify floor plate and ventral neuronal progenitors in the vertebrate neural tube. *Genes Dev.* **24**, 1186-1200.

Rohatgi, R., Milenkovic, L. and Scott, M. P. (2007). Patched1 regulates hedgehog signaling at the primary cilium. *Science* **317**, 372-376.

Rohatgi, R., Milenkovic, L., Corcoran, R. B. and Scott, M. P. (2009). Hedgehog signal transduction by Smoothened: pharmacologic evidence for a 2-step activation process. *Proc. Natl. Acad. Sci. USA* **106**, 3196-3201.

Santos, N. and Reiter, J. F. (2014). A central region of Gli2 regulates its localization to the primary cilium and transcriptional activity. *J. Cell Sci.* **127**, 1500-1510.

Svärd, J., Heby-Henricson, K., Persson-Lek, M., Rozell, B., Lauth, M., Bergström, A., Ericson, J., Toftgård, R. and Teglund, S. (2006). Genetic elimination of Suppressor of fused reveals an essential repressor function in the mammalian Hedgehog signaling pathway. *Dev. Cell* **10**, 187-197.

Taipale, J., Chen, J. K., Cooper, M. K., Wang, B., Mann, R. K., Milenkovic, L., Scott, M. P. and Beachy, P. A. (2000). Effects of oncogenic mutations in Smoothened and Patched can be reversed by cyclopamine. *Nature* **406**, 1005-1009.

Tukachinsky, H., Lopez, L. V. and Salic, A. (2010). A mechanism for vertebrate Hedgehog signaling: recruitment to cilia and dissociation of SuFu-Gli protein complexes. *J. Cell Biol.* **191**, 415-428.

Tuson, M., He, M. and Anderson, K. V. (2011). Protein kinase A acts at the basal body of the primary cilium to prevent Gli2 activation and ventralization of the mouse neural tube. *Development* **138**, 4921-4930.

Wang, Y., Zhou, Z., Walsh, C. T. and McMahon, A. P. (2009). Selective translocation of intracellular Smoothened to the primary cilium in response to Hedgehog pathway modulation. *Proc. Natl. Acad. Sci. USA* **106**, 2623-2628.

Wang, C., Pan, Y. and Wang, B. (2010). Suppressor of fused and Spop regulate the stability, processing and function of Gli2 and Gli3 full-length activators but not their repressors. *Development* **137**, 2001-2009.

Wen, X., Lai, C. K., Evangelista, M., Hongo, J.-A., de Sauvage, F. J. and Scales, S. J. (2010). Kinetics of hedgehog-dependent full-length Gli3 accumulation in primary cilia and subsequent degradation. *Mol. Cell. Biol.* **30**, 1910-1922.

Wilson, C.-W., Chen, M.-H. and Chuang, P.-T. (2009). Smoothened adopts multiple active and inactive conformations capable of trafficking to the primary cilium. *PLoS ONE* **4**, e5182.

Ye, X. and Liu, A. (2011). Hedgehog signaling: mechanisms and evolution. *Front. Biol.* **6**, 504-521.

Zeng, H., Hoover, A. N. and Liu, A. (2010a). PCP effector gene Inturned is an important regulator of cilia formation and embryonic development in mammals. *Dev. Biol.* **339**, 418-428.

Zeng, H., Jia, J. and Liu, A. (2010b). Coordinated translocation of mammalian Gli proteins and suppressor of fused to the primary cilium. *PLoS ONE* **5**, e15900.